We are IntechOpen,
the world's leading publisher of
Open Access books
Built by scientists, for scientists

6,900
Open access books available

186,000
International authors and editors

200M
Downloads

Our authors are among the

154
Countries delivered to

TOP 1%
most cited scientists

12.2%
Contributors from top 500 universities

CLARIVATE ANALYTICS
BOOK CITATION INDEX
INDEXED

WEB OF SCIENCE™

Selection of our books indexed in the Book Citation Index
in Web of Science™ Core Collection (BKCI)

Interested in publishing with us?
Contact book.department@intechopen.com

Numbers displayed above are based on latest data collected.
For more information visit www.intechopen.com

Chapter

Strength Analysis and Variation of Elastic Properties in Plantain Fiber/Polyester Composites for Structural Applications

Christian Emeka Okafor and Christopher Chukwutoo Ihueze

Abstract

Plantain fiber-reinforced composite materials have demonstrated significant properties that are applicable in structural design and development. However, two major concerns arise in relation to the obvious material anisotropy and challenges imposed by structural discontinuity encountered as need for use of fasteners arises. The study assesses the extent of variation of elastic properties (E_x, E_y, G_{xy}, v_{xy}, v_{yx}, m_x, m_y) with fiber orientation using MATLAB functions while considering the extent of variation of the tangential stresses around an idealized functional hole edge. The tensile strength of 410.15 and 288.1 MPa was recorded at 0° fiber orientation angle, while 37.3397 and 33.133 MPa were obtained at fiber orientation angle of 90° for Plantain Empty Fruit Bunch Fiber Composite (PEFBFC) and Plantain Pseudo Stem Fiber Composite (PPSFC), respectively. The tangential stress distribution at hole edge indicated maximum stress value of 119.15 and 100.587 MPa at angular position ø = 90° for PEFBFC and PPSFC, respectively. Judging from various failure indices considered, failure will be initiated at ø = 70° for PEFBFC with stress concentration factor of 2.53 and ø = 65° for PPSFC with stress concentration factor of 2.13, which are less than the stress concentration around the peak stress when angular position is 90°. Both PEFBFC and PPSFC showed similar trends in response to the design scenario considered.

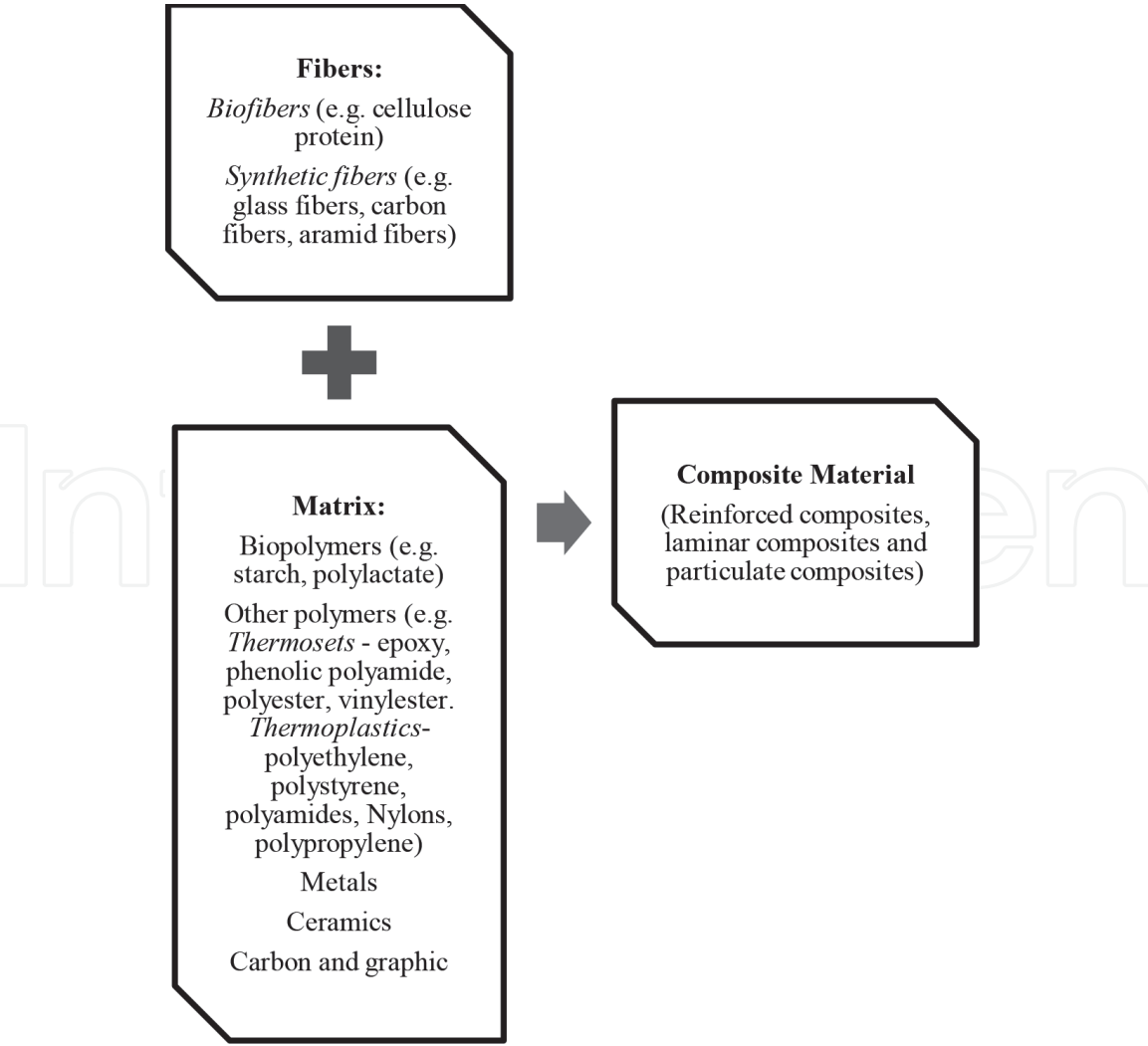**Keywords:** elastic properties, structural application, plantain fiber, composites, matrix

1. Introduction

These days several shortcomings have been observed with respect to the utilization of synthetic fiber-reinforced polymers, hence empowering the drive for more utilization of plant fiber composite in structural designs. The primary weaknesses of synthetic fiber-reinforced polymers which includes issue in afterlife disposal and non-biodegradability are completely settled by utilizing plant fibers in polymer reinforcements. Reinforced composites are prime choice for light weight structural designs and automotive body parts assembly.

Extensive literature on recent advancements in reinforced composites and its reliability are reported in classical reports of Dehmous et al. [1], Okafor et al. [2],

Xie and Wang [3], Beaumont et al. [4], Pei et al. [5], Bittrich et al. [6], Prasad et al. [7], Wang et al. [8]. The hygrothermal efficiencies has been reported by Foulc et al. [9], Shettar et al. [10]. In addition, the utilization of reinforced composites predicates the reuse of domestic and agricultural residues. For example, vehicles made with fiber-reinforced composites are lighter and run on smaller engines which produce fewer emissions to the environment. Most items produced using natural fiber composites is a win-win for manufacturers. Most composite material ventures can utilize their genius green item data to build deals because customers comprehend the ecological dangers of synthetic assembling.

Due to scarcely available information regarding some new material response to structural discontinuity, superior properties of those composites are seriously compromised by the utilization of bizarrely enormous factor of safety in design. Accordingly, the quick fate of composite materials as a class of innovative materials may depend more on clear assessment of its performance in various structural design scenario. All inclusive acknowledgment of composites as eco-friendly materials will therefore depend especially on the certainty of the designer and client about the variation of its elastic properties. In a typical fiber-reinforced composites, the polymer matrix serves as a binder and deforming most times for stress distribution purposes. There are different options in the choice of matrix/fibers and the general composition of reinforced composites is shown in **Figure 1**. The figure identified the three major categories of polymers to include biopolymers, thermoplastics and thermosets. Biopolymers are chain like atoms created by organic

Fibers:

Biofibers (e.g. cellulose protein)

Synthetic fibers (e.g. glass fibers, carbon fibers, aramid fibers)

Matrix:

Biopolymers (e.g. starch, polylactate)

Other polymers (e.g. *Thermosets* - epoxy, phenolic polyamide, polyester, vinylester. *Thermoplastics*- polyethylene, polystyrene, polyamides, Nylons, polypropylene)

Metals

Ceramics

Carbon and graphic

Composite Material

(Reinforced composites, laminar composites and particulate composites)

Figure 1.
Composition of reinforced composites.

biomass. Exceptional nontoxicity and biodegradable properties of biopolymers boosts their applications in composites formulation, hardware and restorative gadgets. Fuse of nano-sized support in the biopolymers to improve the properties contributes to the upgrade functional applications of the matrix.

Though thermosets and thermoplastics sound similar, they have very different properties and applications [11]. Thermosets typically changes from fluid to solid state after curing chemical reaction initiated by addition of a catalyst, cross-linker, and curing agent. In the course of the chemical reaction, the material solidifies as a result of cross-linking and formation of longer molecular networks. Subsequently, any further exposure to high heat will cause the material to degrade unlike thermoplastic parts that melts and softens whenever exposed to elevated temperature, thermoset simply become set in their physical and mechanical properties after an initial treatment and therefore are no longer affected by additional heat exposure.

Again, thermoplastics are dissolvable plastics. At temperature above liquefying point, the thermoplastic condenses. The thermoplastic sets once again into solid state when the temperature is reduced and the handling temperature dips under its melting point. This inherent characteristic of thermoplastics enables its softening when heated above its melting point and re-forming as the temperature decreases below the melting point. Most of the times, the expenses of materials for creating thermoset are lower when contrasted with thermoplastic. Also thermoset is regularly simple for wetting the reinforcements and shaping last composites items. Thermoplastics will in general be harder than thermosets and require no refrigeration as uncured thermosets as often as possible do, and can be more effectively be reused and fixed. Elastomers are typically thermosets (requiring vulcanization).

Obviously literature has indicated several approximate relationships between some reinforced composites elastic constants and the homogenized modules of elasticity [12–14]. Also recent research have reported the possibility of measuring variation elastic constants of materials using ultrasonic methods [15–18]. However, scanty research is available on strength analysis and variation of elastic properties in plantain fiber/polyester composites, a gap that the present study seeks to fill.

2. Background to plantain cultivation and utilization as reinforcement in polymer composites

An expanded enthusiasm for the utilization of agricultural wastes in development of reinforced composites has been on the increase. Natural fibers extracted from bio wastes offer a few points of interest over woody biomass, since they are accessible in huge amounts as leftovers and agricultural wastes [19, 20]. The plantain pseudo stem (PPS) and empty fruit bunch (EFB) strands presented in this chapter are agricultural by-products that are biodegradable and locally available from renewable agricultural sources with potentials to contribute to reduction in environmental pollution when utilized in large scale as polymeric reinforcements.
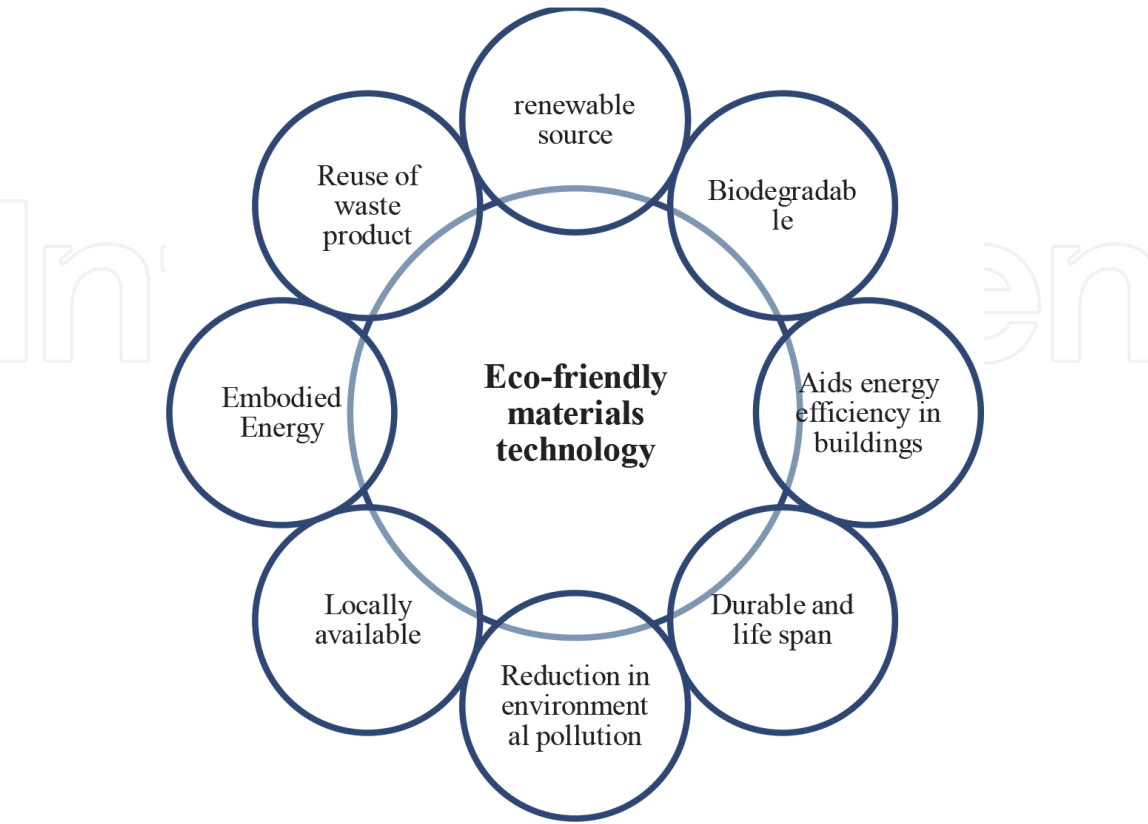
Plantain fruit is one of the staples in Nigeria and it is mainly cultivated in the tropics and ethnic enclaves [21]. It is evaluated that 70 million individuals in West and Central Africa derive most of their nourishment and vitality requirements from plantain fruit plant [22, 23]. Plantain fruit has a fare potential in the light of its huge cultivation and consumption in Nigeria and many other African countries. Akinyemi et al. [24] reported that plantain plant is the third most important plant grown after cassava and yam in Nigeria; collaborating, Kaine and Okoje [25] showed that plantain production is a very profitable enterprise as every ₦1 naira invested in plantain production yields a return on investment of about ₦12.60 kobo. In a study about economics of plantain production Kainga et al. [26] found that the

associated high return on investment and short maturity period for plantain contributes to its massive cultivation in Nigeria.

Africa cultivates over 50% of worldwide production of plantain and Nigeria is one of the biggest plantain producing nations in the planet. Therefore the interest in plantain plant fiber for polymer reinforcement was as a result of its abundance and accessibility as it is evaluated that over 15.07 million tons of plantain fruit is produced each year in Nigeria with about 2.4 million metric tons produced from southern Nigeria [27, 28]. Plantain fiber also satisfied over 50% conditions for eco-friendly materials as shown in **Figure 2** and can make strong reinforcement in composites. A composite which can be characterized as a physical blend of at least two unique materials, has properties that are commonly superior to those of any of the establishing materials. It is important to utilize blends of materials to tackle issues in light of the fact that any one material alone cannot suffix effectively in eco-friendly materials technology at an acceptable performance [29].

Cadena Ch et al. [30] and Adeniyi et al. [31] orchestrated the potentials of natural fibers from plantain pseudo stem for use in fiber-reinforced composites. It is therefore important to assess the extent of variation of elastic properties in plantain fiber-reinforced polyester composites to guard against out of plane failure during structural applications. Unfortunately most studies involving plantain fiber-reinforced composites has dwelt on assessment of tensile, flexural and hardness properties [32], optimization of hardness strengths [33], effect of water and organic extractives removal [34], effects of fiber extraction techniques [35], optimization of flexural strength [36], compressive and impact strength evaluation [37–39], effect of high-frequency microwave radiation [40], effect of chemical treatment on the morphology [41], implications of interfacial energetics on mechanical strength [42]. Although Ihueze, Okafor and Okoye [43] has reported the longitudinal (1) and transverse (2) properties of plantain fiber-reinforced composites in **Figure 1**, there is still need to

Figure 2.
Properties of eco-friendly building materials.

establish the essential elastic constants at directions other than the material axis directions 1–2.

The present research efforts will further drive the interests of structural designers in the use of plantain fiber-reinforced composites because the superior strength of materials are rarely utilized to full as a result of incomplete knowledge of elastic properties which are related to various fundamental solid-state characteristics of the composites. In essence, the elastic constants of plantain fiber-reinforced composites is expected to describe the material response to external stressor and provide useful information about bonding characteristics and structural stability. Kenedi et al. [44] assessed the orthotropic elastic properties in a sandwiched composites laminates and proposed models for estimating the orthotropic elastic properties of composite materials. Hwang and Liu [45] reported that elastic modulus and Poisson's ratio vary significantly with different braid angles in carbon fabric/polyurethane composites. Ren et al. [46] reported that elastic modulus and tensile strengths are overly dependent on the angles of fiber orientation. Kumar et al. [47] studied the influence of $\pm 0°$, $\pm 10°$, $\pm 30°$, $\pm 40°$, $\pm 45°$, $\pm 55°$, $\pm 65°$, $\pm 75°$, and $\pm 90°$ angle ply on mechanical properties of glass-polyester composite laminate and found that that glass/polyester with 0° fiber orientation angle yields' high strength. Cordin et al. [48] experimentally examined the effect of $0°$, $\pm 22.5°$, $\pm 45°$, $\pm 67.5°$ and 90° fiber orientation angles on the mechanical properties of polypropylene-lyocell composites. Ihueze et al. [49] optimally determined the tensile strengths of plantain fiber-reinforced composites considering 30°, 45° and 90° fiber orientation angles. The application of these previous studies are limited to fiber orientation angles studied, however failure may be initiated from angles other than those considered hence the need to verify the variation of important elastic constants within a wide range of fiber orientation coverage are necessary.

Additionally, researchers have provided various theoretical strategies for determination of elastic constants in reinforced composites using software codes to cover the wide range of fabricating conditions. Jules et al. [50] ascertained the effect of fibers orientation on the predicted elastic properties of long fiber composites using Monte-Carlo simulation to assign the in plane and out of plane orientation values. Venetis and Sideridis [51] developed a model to find the approximate elastic constants in unidirectional fiber-reinforced composite materials in terms of the constituent material properties. Cuartas [52] theoretically determined the elastic properties in CFRP composites which compared favorably with other methods based on tensile tests and ultrasonic characterization. Rahmani et al. [12] found that MATLAB codes are capable of predicting the elastic constants of composites with reasonable confidence.

3. Mathematical framework for assessment of extent of variation of elastic properties in plantain fiber-reinforced polyester composites

One significant property of composite materials is their plainly visible macroscopic anisotropy, which means that the properties estimated in the longitudinal direction are by far not the same as those measured in transverse direction. There are no material planes of symmetry, and normal loads create both normal strains and shear strains. This anisotropic characteristic of reinforced composites results in low mechanical properties in the out-of-plane orientation where the matrix carries the primary load. Consequently the application of reinforced composites is limited in scenarios prone to complex load paths such as lugs and fittings [53].

By implication any endeavor to comprehend the structural application of plantain fiber-reinforced polyester composite must assess the inborn anisotropy.

Composites are a subclass of anisotropic materials that are delegated orthotropic. Orthotropic materials have properties that are unique in three directions with perpendicular axes of symmetry. In this way, orthotropic mechanical properties depend heavily on fiber orientation. An orthotropic ply is thus defined as that having two different material properties in two mutually perpendicular directions at a point and the two mutually perpendicular directions also form the planes of material properties symmetry at the point.

3.1 Determination of reduced stiffness matrix and compliance matrix

Considering two possible loading conditions of longitudinal (direction 1) and transverse (direction 2) in the matrix as shown in **Figure 3**, the resulting direct strains from Hooks law are respectively $e_1 = \frac{-v_{21}\sigma_1}{E_1}$ and $e_2 = \frac{-v_{12}\sigma_1}{E_1}$ where v_{12} = major Poisson's ratio and v_{21} = minor Poisson's ratio.

Hence the application of both direct stresses σ_1 and σ_2 will yield corresponding strains as follows:

$$e_1 = \frac{\sigma_1}{E_1} - \frac{v_{21}\sigma_2}{E_2} \tag{1}$$

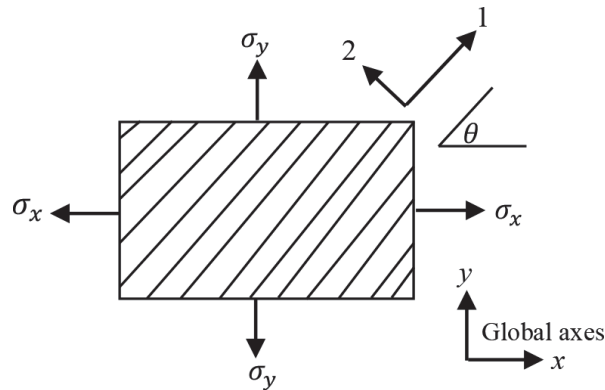$$e_2 = \frac{\sigma_2}{E_2} - \frac{v_{12}\sigma_1}{E_1} \tag{2}$$

Putting Eqs. (1) and (2) in a matrix form, yields

$$\begin{Bmatrix} e_1 \\ e_2 \end{Bmatrix} = \begin{Bmatrix} \dfrac{1}{E_1} & \dfrac{-v_{21}}{E_2} \\ \dfrac{-v_{12}}{E_1} & \dfrac{1}{E_2} \end{Bmatrix} \begin{Bmatrix} \sigma_1 \\ \sigma_2 \end{Bmatrix} \tag{3}$$

$$\begin{Bmatrix} \sigma_1 \\ \sigma_2 \end{Bmatrix} = \begin{Bmatrix} \dfrac{E_1}{1 - v_{12}v_{21}} & \dfrac{v_{21}E_1}{1 - v_{12}v_{21}} \\ \dfrac{v_{12}E_2}{1 - v_{12}v_{21}} & \dfrac{E_2}{1 - v_{12}v_{21}} \end{Bmatrix} \begin{Bmatrix} e_1 \\ e_2 \end{Bmatrix} \tag{4}$$

Eq. (3) is symetric about the loading diagonal such that

$$\frac{-v_{21}}{E_2} = \frac{-v_{12}}{E_1} \tag{5}$$

Figure 3.
Stressed single thin composite lamina. From Ref. [43].

A combined effect of shear and direct stresses gives the reduced stiffness matrix as in Eq. (6) and reduced compliance matrix as in Eq. (7)

$$
\begin{Bmatrix} \sigma_1 \\ \sigma_2 \\ \tau_{12} \end{Bmatrix} = \begin{Bmatrix} \dfrac{E_1}{1 - v_{12}v_{21}} & \dfrac{v_{21}E_1}{1 - v_{12}v_{21}} & 0 \\ \dfrac{v_{12}E_2}{1 - v_{12}v_{21}} & \dfrac{E_2}{1 - v_{12}v_{21}} & 0 \\ 0 & 0 & G_{12} \end{Bmatrix} \begin{Bmatrix} e_1 \\ e_2 \\ e_{12} \end{Bmatrix} \tag{6}
$$

$$
\begin{Bmatrix} e_1 \\ e_2 \\ e_{12} \end{Bmatrix} = \begin{Bmatrix} \dfrac{1}{E_1} & \dfrac{-v_{21}}{E_2} & 0 \\ \dfrac{-v_{21}}{E_1} & \dfrac{1}{E_2} & 0 \\ 0 & 0 & \dfrac{1}{G_{12}} \end{Bmatrix} \begin{Bmatrix} \sigma_1 \\ \sigma_2 \\ \tau_{12} \end{Bmatrix} \tag{7}
$$

Minor Poisson's ratio is the strain resulting from a stress in the axial direction, Ihueze et al. (2013) calculated the major Poisson's ratio v_{12} for plantain fiber/polyester composites. However, there is need to further assess the minor Poisson's ratio v_{21} using Eq. (5) and **Table 1** as follows

$$
v_{21, \text{ PEFBFRP}} = \frac{E_2 v_{12}}{E_1} = \frac{7030.962 * 0.38}{14,922} = 0.179
$$

$$
1 - v_{12}v_{21} = 1 - 0.38 * 0.179 = 1 - 0.068 = 0.93
$$

$$
v_{21, \text{ PPSFC}} = \frac{E_2 v_{12}}{E_1} = \frac{6817.175 * 0.29}{13027.5} = 0.152
$$

$$
1 - v_{12}v_{21} = 1 - 0.29 * 0.152 = 1 - 0.068 = 0.956
$$

The reduced stiffness matrix (ℵ) for PEFBFC and PPSFC is obtained from Eq. (6).
For PEFBFC

$$
\frac{E_1}{1 - v_{12}v_{21}} = \frac{14922}{1 - 0.38 * 0.179} = 16011.07
$$

$$
\frac{v_{21}E_1}{1 - v_{12}v_{21}} = 0.179 * 16011.07 = 2865.98
$$

$$
\frac{E_2}{1 - v_{12}v_{21}} = \frac{7030.962}{1 - 0.38 * 0.179} = 7544.113
$$

Composites	Properties								
	S_{u1} (MPa)	S_{u2} (MPa)	S_y (MPa)	E_1 (MPa)	E_2 (MPa)	E (MPa)	v_{12}	τ_{max} (MPa)	G_{12} (MPa)
PEFBFC	410.15	37.3397	33.69	14,922	7030.962	9990.10	0.38	19.3100	3622.99
PPSFC	288.10	33.1330	29.24	13027.5	6817.175	9146.305	0.29	15.5700	3332.835

S_{u1}, S_{u2} are tensile strengths in the longitudinal and transverse directions respectively.

Table 1.
Evaluated mechanical properties of plantain fibers and plantain fibers reinforced polyester composites. From Ref. [43].

$$\aleph_{\text{PEFBFC}} = \left\{ \begin{array}{ccc} 16011.07 & 2865.98 & 0 \\ 2865.98 & 7544.113 & 0 \\ 0 & 0 & 3622.99 \end{array} \right\} \text{MPa}$$

For PPSFC

$$\frac{E_1}{1 - v_{12}v_{21}} = \frac{13027.5}{1 - 0.29 * 0.152} = 13628.23$$

$$\frac{v_{21}E_1}{1 - v_{12}v_{21}} = 0.152 * 13628.23 = 2071.49$$

$$\frac{E_2}{1 - v_{12}v_{21}} = \frac{6817.175}{1 - 0.29 * 0.152} = 7131.53$$

$$\aleph_{\text{PPSFC}} = \left\{ \begin{array}{ccc} 13628.23 & 2071.49 & 0 \\ 2071.49 & 7131.53 & 0 \\ 0 & 0 & 3332.835 \end{array} \right\} \text{MPa}$$

The reduced compliance matrix (β) is obtained from Eq. (7).
For PEFBFC

$$\frac{1}{E_1} = \frac{1}{14922} = 6.7 \times 10^{-5} 1/\text{MPa}$$

$$\frac{-v_{21}}{E_2} = \frac{-0.179}{7030.962} = -2.5 \times 10^{-5} 1/\text{MPa}$$

$$\frac{1}{E_2} = \frac{1}{7030.962} = 1.4 \times 10^{-4} 1/\text{MPa}$$

$$\frac{1}{G_{12}} = \frac{1}{3622.99} = 2.8 \times 10^{-4} 1/\text{MPa}$$

$$\beta_{\text{PEFBFC}} = \left\{ \begin{array}{ccc} 6.7 \times 10^{-5} & -2.5 \times 10^{-5} & 0 \\ -2.5 \times 10^{-5} & 1.4 \times 10^{-4} & 0 \\ 0 & 0 & 2.8 \times 10^{-4} \end{array} \right\} 1/\text{MPa}$$

For PPSFC

$$\frac{1}{E_1} = \frac{1}{13027.5} = 7.7 \times 10^{-5} 1/\text{MPa}$$

$$\frac{-v_{21}}{E_2} = \frac{-0.152}{6817.175} = -2.2 \times 10^{-5} 1/\text{MPa}$$

$$\frac{1}{E_2} = \frac{1}{6817.175} = 1.5 \times 10^{-4} 1/\text{MPa}$$

$$\frac{1}{G_{12}} = \frac{1}{3332.835} = 3.0 \times 10^{-4} 1/\text{MPa}$$

$$\beta_{\text{PPSFC}} = \left\{ \begin{array}{ccc} 7.7 \times 10^{-5} & -2.2 \times 10^{-5} & 0 \\ -2.2 \times 10^{-5} & 1.5 \times 10^{-4} & 0 \\ 0 & 0 & 3.0 \times 10^{-4} \end{array} \right\} 1/\text{MPa}$$

Property	Polyester resin
Density (g/cm³)	1.2–1.5 (1400 kg/m³)
Young modulus (MPa)	2000–4500
Tensile strength (MPa)	40–90
Compressive strength (MPa)	90–250
Tensile elongation at break (%)	2
Water absorption 24 h at 20°C	0.1–0.3
Flexural modulus (GPa)	11.0
Poisson's ratio	0.37–0.38
	Plantain pseudo stem fibers
Young modulus (MPa)	23,555
UTS (MPa)	536.2
Strain (%)	2.37
Density (kg/m³)	381.966
	Plantain empty fruit bunch fibers
Young modulus (MPa)	27,344
UTS (MPa)	780.3
Strain (%)	2.68
Density (kg/m³)	354.151

Table 2.
Mechanical properties of plantain fibers and polyester resin. From Ref. [43].

3.2 Transformation of elastic constants

The know of the stress-strain relationship in the plantain/polyester composite is completely comprehended by knowing the associated independent engineering elastic constants (E_1, E_2, G_{12} and v_{12}) as previously determined by Ihueze et al. (2013) as in **Tables 1** and **2**. However, there is need to further establish these elastic properties at different directions of fibers other than directions 1 and 2. Datoo [54] derived various expressions for determination of the elastic properties in the reference axes *x-y* for any fiber orientation as expressed in Eqs. (8)–(14) where $c = cos\theta$, $s = sin\theta$, E_x, E_y, G_{xy}, v_{xy}, m_x and m_y are the elastic properties at any fiber orientation θ relative to a reference direction *x-y*.

$$\frac{1}{E_x} = \frac{c^4}{E_1} + \frac{s^4}{E_2} + c^2s^2\left(\frac{1}{G_{12}} - \frac{2v_{12}}{E_1}\right) \qquad (8)$$

$$\frac{1}{E_y} = \frac{s^4}{E_1} + \frac{c^4}{E_2} + c^2s^2\left(\frac{1}{G_{12}} - \frac{2v_{12}}{E_1}\right) \qquad (9)$$

$$\frac{1}{G_{xy}} = c^2s^2\left(\frac{4}{E_1} + \frac{4}{E_2} + \frac{8v_{12}}{E_1}\right) + \left(c^2 - s^2\right)\frac{1}{G_{12}} \qquad (10)$$

$$v_{xy} = E_x\left[\left(c^4 + s^4\right)\frac{v_{12}}{E_1} - c^2s^2\left(\frac{1}{E_1} + \frac{1}{E_2} - \frac{1}{G_{12}}\right)\right] \qquad (11)$$

The minor Poissons ratio with respect to the material reference axes is obtained from Eq. (5) such that

$$\frac{v_{xy}}{E_x} = \frac{v_{yx}}{E_y} \tag{12}$$

$$m_x = E_x \left[c^3 s \left(\frac{1}{G_{12}} - \frac{2v_{12}}{E_1} - \frac{2}{E_1} \right) - cs^3 \left(\frac{1}{G_{12}} - \frac{2v_{12}}{E_1} - \frac{2}{E_2} \right) \right] \tag{13}$$

$$m_y = E_y \left[cs^3 \left(\frac{1}{G_{12}} - \frac{2v_{12}}{E_1} - \frac{2}{E_1} \right) - c^3 s \left(\frac{1}{G_{12}} - \frac{2v_{12}}{E_1} - \frac{2}{E_2} \right) \right] \tag{14}$$

3.3 Variation of engineering elastic constants with fiber orientation θ

Considering fiber orientation $\theta°$ ranging from 0° to 90° in increments of 5° the variation of E_x, E_y, G_{xy}, v_{xy}, m_x and m_y has been assessed Plantain Empty Fruit Bunch Fiber Composite (PEFBFC) and Plantain Pseudo Stem Fiber Composite (PPSFC) using Eqs. (8)–(14) and presented in **Tables 3** and **4**, respectively.
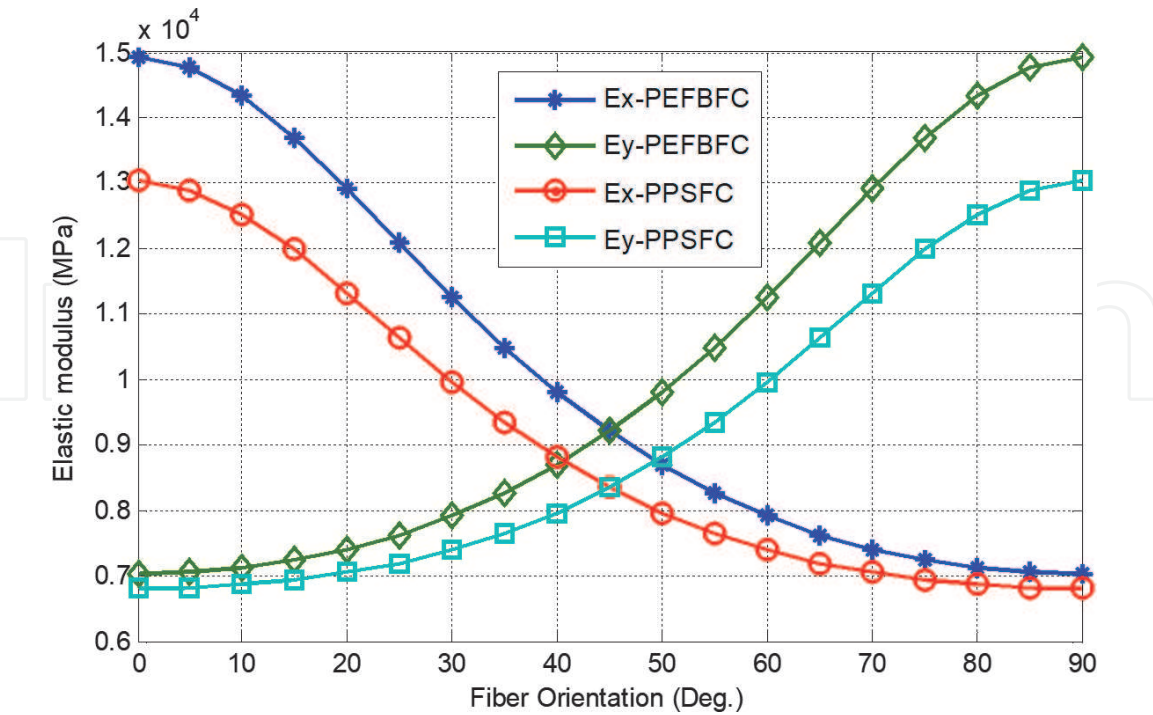
Figure 4 shows the variation of elastic modulus with fiber orientation, it can be seen that the highest value of 14,922 and 13027.5 MPa in the reference x-direction (E_x) is attained in the fiber orientation angle 0° for PEFBFC and PPSFC respectively. However as fiber orientation angle changes, there is a sharp drop in the value of elastic modulus in the reference x-direction to a respective lowest value of 7030.96 and 6817.18 MPa as the fiber orientation angle increased to 90°. On the contrary, the lowest value of 7030.96 and 6817.18 MPa were recorded for elastic modulus in the

S/N	$\theta°$	E_x	E_y	G_{xy}	v_{xy}	v_{yx}	m_x	m_y	$\frac{E_x}{E_2}$	$\frac{G_{xy}}{E_2}$
1	0	14922.000	7030.962	3622.990	0.380	0.179	0.000	0.000	2.122	0.515
2	5	14769.770	7053.373	3629.270	0.378	0.180	0.116	0.037	2.101	0.516
3	10	14337.670	7121.323	3647.477	0.372	0.185	0.221	0.073	2.039	0.519
4	15	13690.480	7236.950	3675.727	0.362	0.191	0.304	0.111	1.947	0.523
5	20	12911.620	7403.786	3710.985	0.350	0.201	0.362	0.150	1.836	0.528
6	25	12081.300	7626.692	3749.256	0.336	0.212	0.395	0.190	1.718	0.533
7	30	11262.730	7911.712	3785.946	0.320	0.225	0.405	0.231	1.602	0.538
8	35	10497.990	8265.787	3816.391	0.304	0.239	0.398	0.271	1.493	0.543
9	40	9810.462	8696.213	3836.528	0.288	0.255	0.377	0.310	1.395	0.546
10	45	9209.655	9209.655	3843.571	0.271	0.271	0.346	0.346	1.310	0.547
11	50	8696.213	9810.462	3836.528	0.255	0.288	0.310	0.377	1.237	0.546
12	55	8265.787	10497.990	3816.391	0.239	0.304	0.271	0.398	1.176	0.543
13	60	7911.712	11262.730	3785.946	0.225	0.320	0.231	0.405	1.125	0.538
14	65	7626.692	12081.300	3749.256	0.212	0.336	0.190	0.395	1.085	0.533
15	70	7403.786	12911.620	3710.985	0.201	0.350	0.150	0.362	1.053	0.528
16	75	7236.950	13690.480	3675.727	0.191	0.362	0.111	0.304	1.029	0.523
17	80	7121.323	14337.670	3647.477	0.185	0.372	0.073	0.221	1.013	0.519
18	85	7053.373	14769.770	3629.270	0.180	0.378	0.037	0.116	1.003	0.516
19	90	7030.962	14922.000	3622.990	0.179	0.380	0.000	0.000	1.000	0.515

Table 3.
Variation of engineering elastic constants with fiber orientation θ *in PEFBFC.*

S/N	$\theta°$	E_x	E_y	G_{xy}	v_{xy}	v_{yx}	m_x	m_y	$\frac{E_x}{E_2}$	$\frac{G_{xy}}{E_2}$
1	0	13027.500	6817.175	3332.835	0.290	0.152	0.000	0.000	1.911	0.489
2	5	12897.620	6830.651	3343.613	0.290	0.154	0.114	0.023	1.892	0.490
3	10	12530.190	6872.014	3375.039	0.291	0.159	0.214	0.047	1.838	0.495
4	15	11983.280	6944.024	3424.350	0.291	0.168	0.293	0.073	1.758	0.502
5	20	11330.960	7051.119	3486.843	0.290	0.180	0.344	0.103	1.662	0.511
6	25	10643.310	7199.198	3555.901	0.287	0.194	0.369	0.136	1.561	0.522
7	30	9974.406	7395.333	3623.334	0.282	0.209	0.371	0.173	1.463	0.532
8	35	9359.192	7647.394	3680.229	0.275	0.224	0.356	0.212	1.373	0.540
9	40	8816.012	7963.509	3718.337	0.265	0.239	0.328	0.252	1.293	0.545
10	45	8351.207	8351.207	3731.758	0.253	0.253	0.292	0.292	1.225	0.547
11	50	7963.509	8816.012	3718.337	0.239	0.265	0.252	0.328	1.168	0.545
12	55	7647.394	9359.192	3680.229	0.224	0.275	0.212	0.356	1.122	0.540
13	60	7395.333	9974.406	3623.334	0.209	0.282	0.173	0.371	1.085	0.532
14	65	7199.198	10643.310	3555.901	0.194	0.287	0.136	0.369	1.056	0.522
15	70	7051.119	11330.960	3486.843	0.180	0.290	0.103	0.344	1.034	0.511
16	75	6944.024	11983.280	3424.350	0.168	0.291	0.073	0.293	1.019	0.502
17	80	6872.014	12530.190	3375.039	0.159	0.291	0.047	0.214	1.008	0.495
18	85	6830.651	12897.620	3343.613	0.154	0.290	0.023	0.114	1.002	0.490
19	90	6817.175	13027.500	3332.835	0.152	0.290	0.000	0.000	1.000	0.489

Table 4.
Variation of engineering elastic constants with fiber orientation θ in PPSFC.

Figure 4.
Variation of elastic modulus with fiber orientation in PEFBFC and PPSFC.

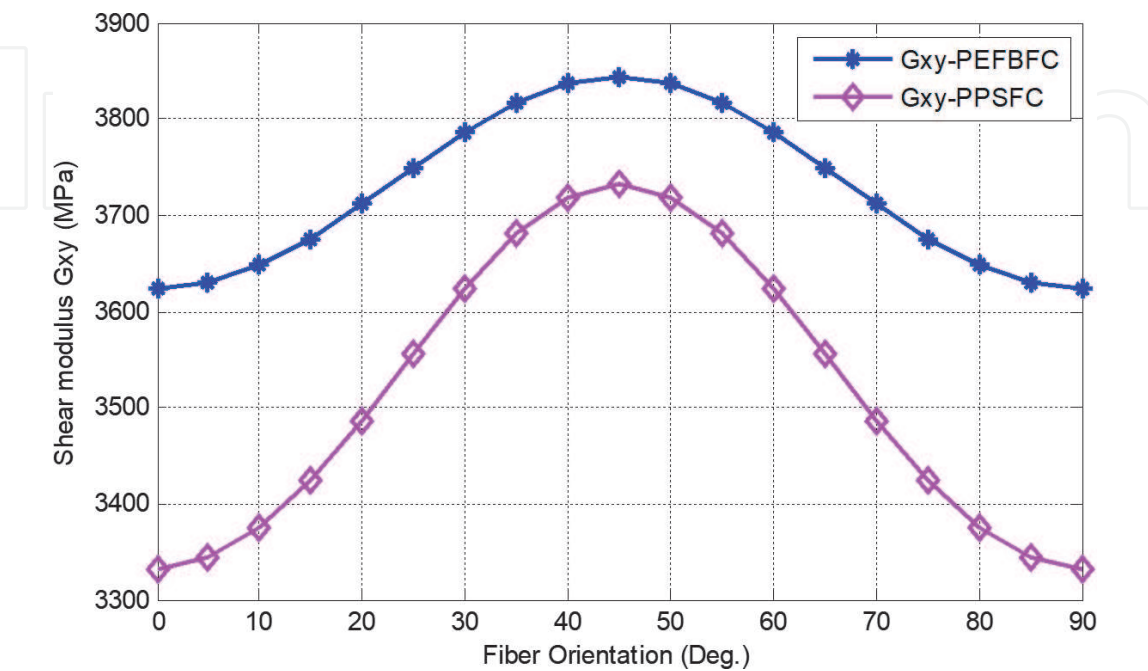reference *y*-direction (E_y) as the fiber orientation angle increased from 0° to 90° reaching a peak value of 14,922 and 13027.5 MPa for PEFBFC and PPSFC respectively. The implication is that reinforcements are required to be aligned in the

direction of applied load [55]. Although Jones [56] intuitively suggested that highest value of material properties may not necessarily occur along the principal material directions, rather it is essential that transverse reinforcement is needed in unidirectional fiber composites which are subjected to multi axial loading [57].

As can be seen in **Figure 5** that shear modulus peaked at 45° fiber orientation and shear modulus was symmetric at about 45° fiber orientation angle for both PEFBFC and PPSFC considered. This implies that the higher in-plane shear resistance is achievable when fiber orientation is 45°. Also the respective minimum value of 3622.99 and 3332.83 MPa at fiber orientation 0° for PEFBFC and PPSFC can be seen to gradually increase to maximum values of 3843.57 and 3731.758 MPa at fiber orientation 45° and then reversed parabolically at 90° where it again reaches to 3622.99 and 3332.84 MPa. Similar trend was obtained by Farooq and Myler [58] who developed efficient procedures for determination of mechanical properties of carbon fiber-reinforced laminated composite panels. This trend in which the value of G_{xy} peaks at 45° fiber orientation angle and lowers at 0° and 90° fiber orientation angle indicates that off-axis reinforcement is very necessary for robust shear stiffness in unidirectional composites [57].
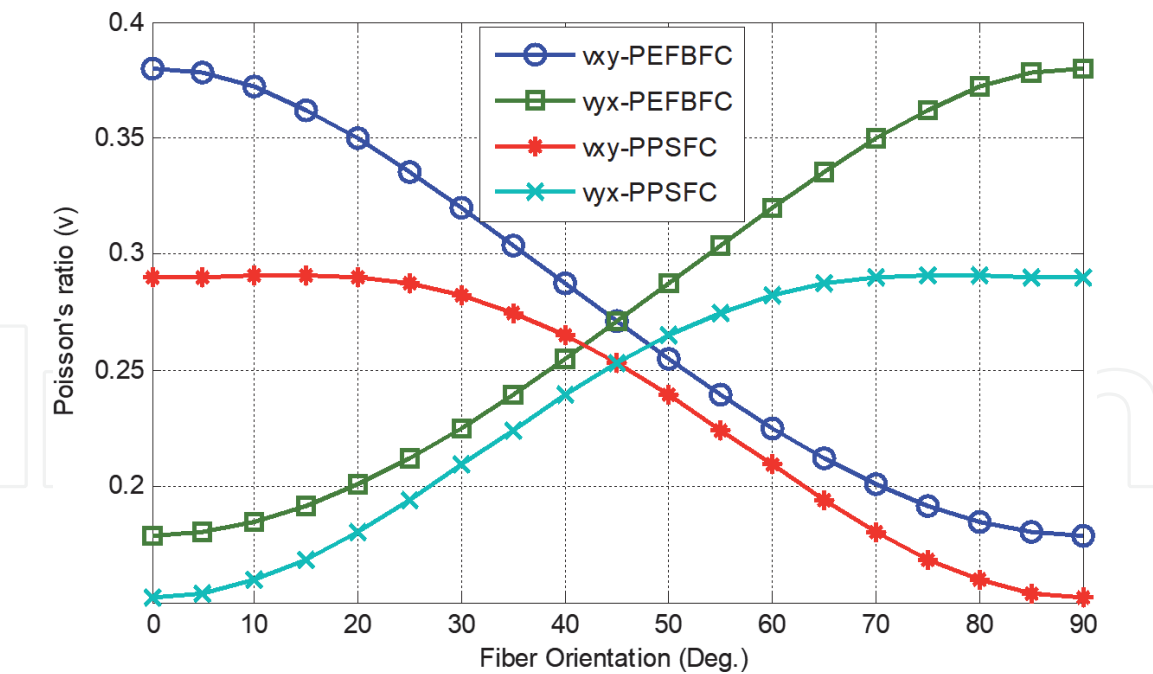
Figure 6 shows variation of Poisson's ratio with fiber orientation, the graph depicts a gradual drop of major Poisson's ratio (v_{xy}) for PEFBFC and PPSFC respectively from 0.38 and 0.29 when fibers are aligned at 0° orientation angle to a lowest value of 0.18 and 0.15 value when fibers were aligned at 90° orientation angle. Additionally, the minor Poissons ratio (v_{yx}) for PEFBFC and PPSFC increased respectively from 0.18 and 0.15 when fibers are aligned at 0° orientation angle to a highest value of 0.38 and 0.29 value when fibers were aligned at 90° orientation angle.

Figure 7 depicts the variation of shear coupling coefficient with fiber orientation, equal magnitude of shear coupling effect was obtained at 45° fiber orientation angle for both PEFBFC and PPSFC considered. Gibson [57] reported that shear coupling coefficient is a measure of the amount of shear strain developed in the *xy* plane per unit normal strain along the direction of the applied normal stress σ_x. **Figure 7** clearly indicate that the maximum value of the shear coupling coefficient in the reference *x*-direction for PEFBFC and PPSFC was attained at 30° fiber orientation angle while the coefficient in the reference *y*-direction for PEFBFC and
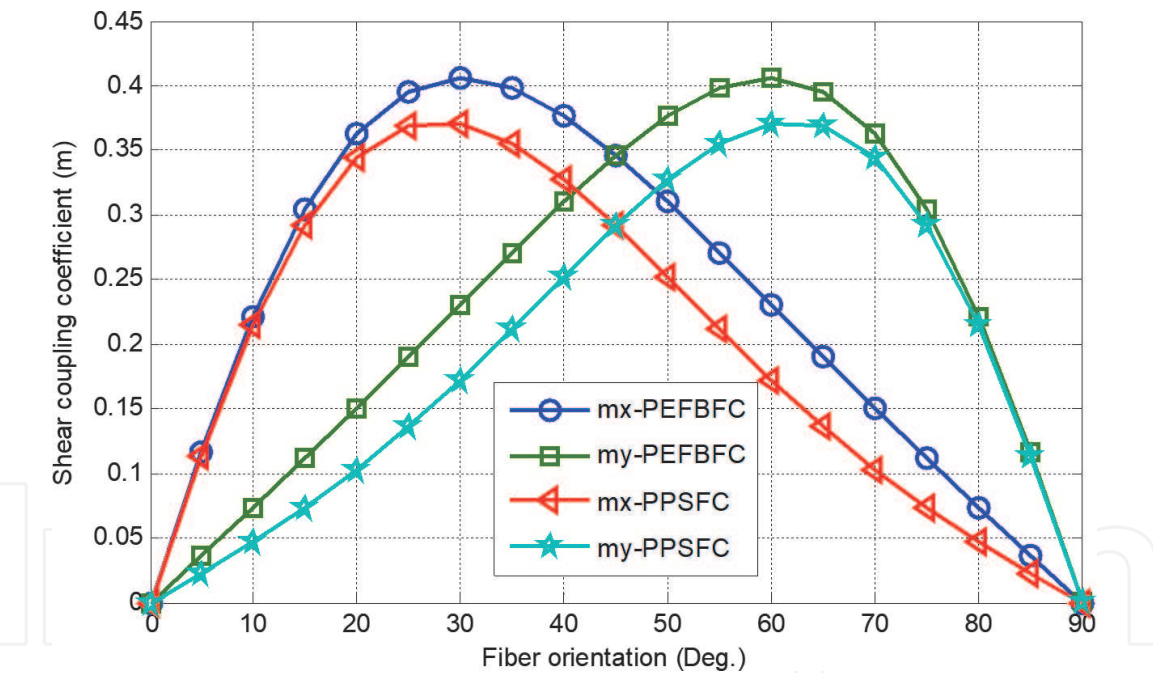

Figure 5.
Variation of shear modulus with fiber orientation in PEFBFC and PPSFC.

Figure 6.
Variation of Poisson's ratio with fiber orientation in PEFBFC and PPSFC.

Figure 7.
Variation of shear coupling coefficient with fiber orientation in PEFBFC and PPSFC.

PPSFC was attained at 60° fiber orientation angle. This is an indication that as the shear-coupling ratio increases, the amount of shear coupling increases.

4. Tsai-Hill failure criteria assessment of longitudinal tensile strength

Failure theory is essential in determining whether the composite has failed. Literature review has shown that results of failure prediction depend on failure criterion applied and one major failure criteria used in the industries is Tsai-Hill and

failure criteria. Additionally, since composites ultimate tensile strength and strain depend on the fiber orientation, a failure criterion must be used in which the applied stress system is also in material axis [54]. Tsai-Hill theory considers an interaction of the stresses in the fiber direction. It postulates that failure can only occur in reinforced composites when the failure index exceeds 1, hence Eq. (19) must be satisfied to avoid failure.

By considering an arbitrary positive angle θ with reference to the *x*-axis in **Figure 3**, Ihueze et al. [43] transformed the stresses within the global axes (*x-y*) into material axes 1–2 as given in Eq. (15)

$$
\begin{Bmatrix} \sigma_1 \\ \sigma_2 \\ \tau_{12} \end{Bmatrix} = \begin{bmatrix} c^2 & s^2 & 2sc \\ s^2 & c^2 & -2sc \\ -sc & sc & (c^2 - s^2) \end{bmatrix} \begin{Bmatrix} \sigma_x \\ \sigma_y \\ \tau_{xy} \end{Bmatrix}
\tag{15}
$$

where $c = cos\theta$ and $s = sin\theta$. Taking longitudinal direction stresses as $\sigma_y = \tau_{xy} = 0$ and thus

$$
\sigma_1 = \sigma_x \cos^2\theta
\tag{16}
$$

$$
\sigma_2 = \sigma_x \sin^2\theta
\tag{17}
$$

$$
\tau_{12} = -\sigma_x \cos\theta \sin\theta
\tag{18}
$$

Considering Tsai-Hill failure criterion and setting the failure index as 1 for the composite failure to occur:

$$
\left(\frac{\sigma_1}{S_{u1}}\right)^2 + \left(\frac{\sigma_2}{S_{u2}}\right)^2 + \left(\frac{\tau_{12}}{\tau_{max}}\right)^2 - \left(\frac{\sigma_1}{S_{u1}}\right)\left(\frac{\sigma_2}{S_{u1}}\right) = 1
\tag{19}
$$

Substituting the appropriate value in Eq. (19) we have for PEFBFC

$$
\left(\frac{\sigma_x \cos^2\theta}{410.15}\right)^2 + \left(\frac{\sigma_x \sin^2\theta}{37.3397}\right)^2 + \left(\frac{-\sigma_x \cos\theta \sin\theta}{19.3100}\right)^2 - \left(\frac{\sigma_x \cos^2\theta}{410.15}\right)\left(\frac{\sigma_x \sin^2\theta}{410.15}\right) = 1
$$

$$
\sigma_{x,\,PEFBFC} = \sqrt{\frac{1}{\left(\cos^4\theta/410.15^2 + \sin^4\theta/37.3397^2 + \cos^2\theta \sin^2\theta/19.3100^2 - \cos^2\theta \sin^2\theta/410.15^2\right)}}
$$

And for PPSFC

$$
\left(\frac{\sigma_x \cos^2\theta}{288.10}\right)^2 + \left(\frac{\sigma_x \sin^2\theta}{33.1330}\right)^2 + \left(\frac{-\sigma_x \cos\theta \sin\theta}{15.5700}\right)^2 - \left(\frac{\sigma_x \cos^2\theta}{288.10}\right)\left(\frac{\sigma_x \sin^2\theta}{288.10}\right) = 1
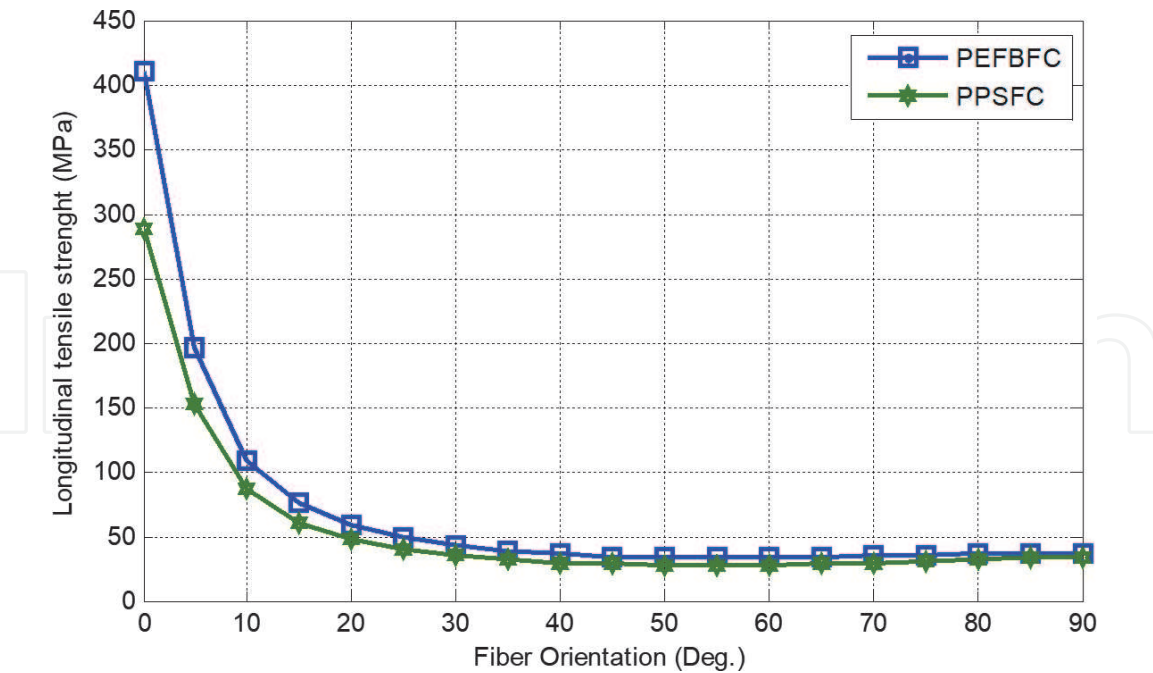$$

$$
\sigma_{x,\,PPSFC} = \sqrt{\frac{1}{\left(\cos^4\theta/288.10^2 + \sin^4\theta/33.1330^2 + \cos^2\theta \sin^2\theta/15.5700^2 - \cos^2\theta \sin^2\theta/288.10^2\right)}}
$$

Hence the value for σ_x is then calculated for orientation ranging from 0° to 90° as shown in **Table 5**.

The variation of longitudinal tensile strength with fiber orientation for PEFBFC and PPSFC has been presented in **Figure 8**, it can be seen that the tensile strength equals 410.15 and 288.1 MPa which are the longitudinal tensile strength for PEFBFC and PPSFC respectively when fiber orientation angle is 0°; on the other hand, the tensile strength equals 37.3397 and 33.133 MPa which are the transverse tensile strength for PEFBFC and PPSFC respectively when fiber orientation angle is 90°.

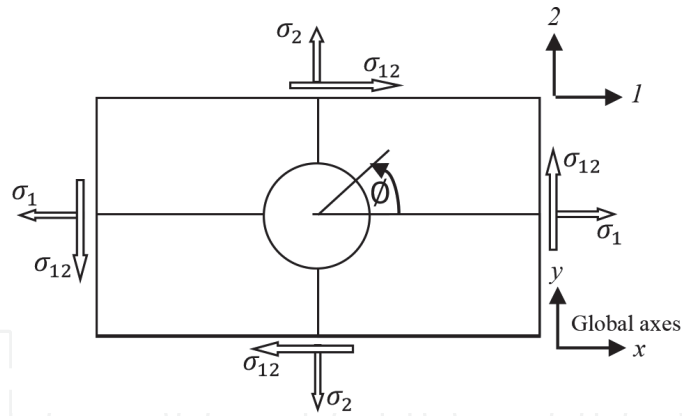| S/N	Orientation θ	PEFBFC	PPSFC
1	0	410.15	288.1
2	5	195.86	152.635
3	10	108.786	86.8937
4	15	75.4556	60.6747
5	20	58.6356	47.3142
6	25	48.8262	39.5106
7	30	42.6439	34.6088
8	35	38.6038	31.4352
9	40	35.9607	29.4005
10	45	34.3043	28.1833
11	50	33.3926	27.5977
12	55	33.0716	27.5303
13	60	33.2311	27.9038
14	65	33.774	28.6492
15	70	34.5913	29.679
16	75	35.5418	30.8595
17	80	36.4447	31.9912
18	85	37.0995	32.8242
19	90	37.3397	33.133

Table 5.
Longitudinal tensile strength variation with fiber orientation angle.

Figure 8.
Variation of longitudinal tensile strength with fiber orientation for PEFBFC and PPSFC.

5. Variation of tangential stress and modulus around a structural discontinuity

Structural discontinuity arising from holes in reinforced composites created for joining or access purposes causes stress concentration at the point of discontinuity [59].

15

Figure 9.
Depiction of hole in the plantain fiber-reinforced composites sample.

Adequate comprehension of stress redistribution pattern and concentrations is helpful for proficient and safe structural designs. Unlike in ductile materials where stress concentration is of no much ado, plantain fiber-reinforced composites may be sufficiently brittle, hence every form of stress concentration and structural discontinuity has to be properly designed. In a typical scenario where a circular hole is created in the composite as shown in **Figure 9**, assuming no interlaminar stresses exist around the free edge of the hole, the ply is nominally stressed by σ_1, σ_2, σ_{12} some distance away from the hole as indicated. Lekhnitskii [60] derived various useful expressions for stress distribution around holes in a composite plate, the tangential elastic modulus $E_\varnothing$ at an angular position $\varnothing$ is determined using Eq. (20).

$$E_\varnothing = \frac{1}{\left(\frac{\sin^4 \varnothing}{E_1} + \left[\frac{1}{G_{12}} - \frac{2v_{12}}{E_1} \right] \sin^2 \varnothing \cos^2 \varnothing + \frac{\cos^4 \varnothing}{E_2} \right)} \tag{20}$$

Hence the tangential stress $\sigma_\varnothing$ at the perifery of the hole with an angle $\varnothing$ is found from Eq. (21).

$$\sigma_\varnothing = \frac{E_\varnothing}{E_1} (A\sigma_1 + B\sigma_2 + C\sigma_{12}) \tag{21}$$

where

$$A = \cos^2 \varnothing + (1 + p) \sin^2 \varnothing$$

$$B = q\{(q + p) \cos^2 \varnothing - \sin^2 \varnothing\}$$

$$C = (1 + q + p)p \sin 2\varnothing$$

$$p = \sqrt{2(q - v_{12}) + \frac{E_1}{G_{12}}}$$

$$q = \sqrt{\frac{E_1}{E_2}}$$

Using the stress transformation matrix and replacing the axes system 1–2 by radial (r)-tangential ($\varnothing$), we can resolve the tangential stress $\sigma_\varnothing$ back into the material axesin Eq. (22) for proper strength evaluation

$$\begin{Bmatrix} \sigma_r \\ \sigma_\varnothing \\ \tau_{r\varnothing} \end{Bmatrix} = \begin{bmatrix} c^2 & s^2 & -2sc \\ s^2 & c^2 & 2sc \\ sc & -sc & (c^2 - s^2) \end{bmatrix} \begin{Bmatrix} \sigma_x \\ \sigma_y \\ \tau_{xy} \end{Bmatrix} \tag{22}$$

At the edge of the hole, only the tangential stress $\sigma_\emptyset > 0$, thus $\sigma_r = \sigma_{r\emptyset} = 0$ in Eq. (22), therefore

$$\sigma_1 = \sigma_x = \sigma_\emptyset \sin^2\emptyset \tag{23}$$

$$\sigma_2 = \sigma_y = \sigma_\emptyset \cos^2\emptyset \tag{24}$$

$$\sigma_{12} = \sigma_{xy} = -\sigma_\emptyset \cos\emptyset \sin\emptyset \tag{25}$$

Using the maximum stress criterion, the material will fail when any stress value in the material axes exceeds their respective ultimate strenght. Such that

$$\left|\frac{\sigma_1}{S_{u1}}\right| < 1 \tag{26}$$

$$\left|\frac{\sigma_2}{S_{u2}}\right| < 1 \tag{27}$$

$$\left|\frac{\sigma_{12}}{\tau_{max}}\right| < 1 \tag{28}$$

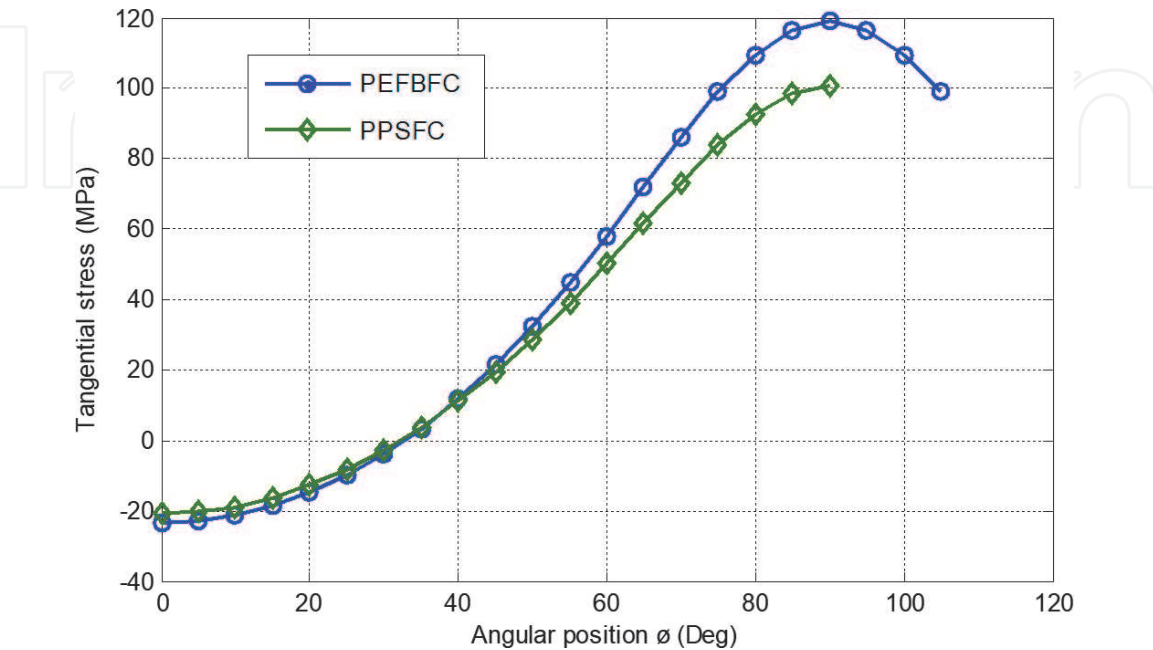| S/N	$E_\emptyset$	$\sigma_\emptyset$	σ_1	σ_2	σ_{12}	F.I.$_1$	F.I.$_2$	F.I.$_{12}$	Stress conc.
0	7030.962	−23.338	0.000	−23.338	0.000	0.000	0.625	0.000	−0.69
5	7053.373	−22.807	−0.173	−22.634	1.980	0.000	0.606	0.103	−0.67
10	7121.323	−21.211	−0.640	−20.571	3.627	0.002	0.551	0.188	−0.62
15	7236.950	−18.542	−1.242	−17.300	4.636	0.003	0.463	0.240	−0.55
20	7403.786	−14.786	−1.730	−13.056	4.752	0.004	0.350	0.246	−0.43
25	7626.692	−9.917	−1.771	−8.146	3.799	0.004	0.218	0.197	−0.29
30	7911.712	−3.903	−0.976	−2.927	1.690	0.002	0.078	0.088	−0.11
35	8265.787	3.303	1.087	2.217	−1.552	0.003	0.059	0.080	0.10
40	8696.213	11.751	4.855	6.896	−5.786	0.012	0.185	0.300	0.35
45	9209.655	21.484	10.742	10.742	−10.742	0.026	0.288	0.556	0.63
50	9810.462	32.515	19.080	13.434	−16.010	0.047	0.360	0.829	0.96
55	10497.994	44.784	30.050	14.733	−21.042	0.073	0.395	1.090	1.32
60	11262.726	58.103	43.577	14.526	−25.159	0.106	0.389	1.303	1.71
65	12081.304	72.076	59.203	12.873	−27.607	0.144	0.345	1.430	2.12
70	12911.622	86.025	75.962	10.063	−27.648	0.185	0.269	1.432	2.53
75	13690.476	98.951	92.323	6.628	−24.738	0.225	0.178	1.281	2.91
80	14337.671	109.599	106.294	3.305	−18.742	0.259	0.089	0.971	3.22
85	14769.765	116.668	115.782	0.886	−10.130	0.282	0.024	0.525	3.43
90	14922.000	119.152	119.152	0.000	0.000	0.291	0.000	0.000	3.50
95	14769.765	116.668	115.782	0.886	10.130	0.282	0.024	0.525	3.43
100	14337.671	109.599	106.294	3.305	18.742	0.259	0.089	0.971	3.22
105	13690.476	98.951	92.323	6.628	24.738	0.225	0.178	1.281	2.91

Table 6.
Variation of tangential stress, material axis stress and tangential modulus at the edge of material discontinuity in PEFBFC.

The left hand side of Eqs. (26)–(28) represents the failure indices (FI). The maximum failure index (FI) for the applied stress is factored in to obtain the load factor. Due to the inherent material orthotropy, the failure zone of the plantain

S/N	$E_\varnothing$	$\sigma_\varnothing$	σ_1	σ_2	σ_{12}	$F.I._1$	$F.I._2$	$F.I._{12}$	Stress conc.
0	6817.175	−20.978	0.000	−20.978	0.000	0.000	0.633	0.000	−0.72
5	6830.651	−20.459	−0.155	−20.304	1.776	0.001	0.613	0.114	−0.71
10	6872.014	−18.909	−0.570	−18.339	3.234	0.002	0.554	0.208	−0.65
15	6944.024	−16.346	−1.095	−15.251	4.086	0.004	0.460	0.262	−0.56
20	7051.119	−12.791	−1.496	−11.295	4.111	0.005	0.341	0.264	−0.44
25	7199.198	−8.269	−1.477	−6.792	3.167	0.005	0.205	0.203	−0.29
30	7395.333	−2.793	−0.698	−2.095	1.209	0.002	0.063	0.078	−0.10
35	7647.394	3.635	1.196	2.439	−1.708	0.004	0.074	0.110	0.13
40	7963.509	11.024	4.555	6.469	−5.428	0.016	0.195	0.349	0.38
45	8351.207	19.391	9.695	9.695	−9.695	0.034	0.293	0.623	0.67
50	8816.012	28.736	16.863	11.873	−14.150	0.059	0.358	0.909	0.99
55	9359.192	39.014	26.179	12.835	−18.331	0.091	0.387	1.177	1.35
60	9974.406	50.087	37.565	12.522	−21.688	0.130	0.378	1.393	1.73
65	10643.308	61.651	50.640	11.011	−23.614	0.176	0.332	1.517	2.13
70	11330.958	73.175	64.615	8.560	−23.518	0.224	0.258	1.510	2.52
75	11983.277	83.856	78.239	5.617	−20.964	0.272	0.170	1.346	2.89
80	12530.185	92.667	89.873	2.794	−15.847	0.312	0.084	1.018	3.20
85	12897.622	98.526	97.778	0.748	−8.554	0.339	0.023	0.549	3.40
90	13027.500	100.587	100.587	0.000	0.000	0.349	0.000	0.000	3.47

Table 7.
Variation of tangential stress, material axis stress and tangential modulus at the edge of material discontinuity in PPSFC.

Figure 10.
Tangential stress distribution at a hole edge for PEFBFC and PPSFC.

fiber-reinforced composite as a result of structural discontinuity may not necessarily occur at the point of maximum stress concentration, therefore it is important to assess the extent of variation of the tangential stress around the hole edge and the failure index using maximum stress theory at other points aside the point of maximum stress concentration. Also in the present consideration we take a simplified scenario where $\sigma_2 = \sigma_{12} = 0$ such that the ply of dimensions $150 \times 19.05 \times 3.2$ mm with a circular hole at the center is subjected to only nominal axial stress $\sigma_{PEFBFC} = 34$ MPa and $\sigma_{PPSFC} = 29$ MPa. **Tables 6** and **7** depict the values of tangential stress, material axis stress and tangential modulus as computed using Eq. (20)–(25).

Tangential stress distribution at hole edge for PEFBFC and PPSFC are shown in **Figure 10**, the maximum stress value of 119.15 and 100.587 MPa was attained at angular position ø = 90° for PEFBFC and PPSFC respectively. However, considering various failure indices in **Tables 5** and **6**, failure will be initiated at ø = 70° for PEFBFC with stress concentration factor of 2.53 and ø = 65° for PPSFC with stress concentration factor of 2.13 which are less than the stress concentration around the peak stress when angular position is 90°.

6. Conclusions

The utilization of plantain fiber-reinforced composites in structural applications empowers architects to acquire huge accomplishments in the usefulness, security and economy of development. These materials have high proportion of strength-to-density ratio, can be tailored to posses certain mechanical properties. The elastic constants of plantain fiber-reinforced composites depend greatly on fiber orientation with notable anisotropic characteristics which makes it less attractive for applications involving lugs and fittings. The present report amplified some notable design procedures in handling such limitations in plantain fiber-reinforced composites using relevant failure theories. Both plantain EFBFRC and PSFRC showed similar trends in response to the design scenario considered. Be that as it may be, a proficient utilization of plantain fiber-reinforced composites in structural applications requires a cautious assessment of all influential factors.

Author details

Christian Emeka Okafor[1*] and Christopher Chukwutoo Ihueze[2]

1 Department of Mechanical Engineering, Nnamdi Azikiwe University, Awka, Nigeria

2 Department of Industrial, Production Engineering, Nnamdi Azikiwe University, Awka, Nigeria

*Address all correspondence to: ce.okafor@unizik.edu.ng

IntechOpen

References

[1] Dehmous H, Welemane H, Karama M, Tahar KA. Reliability approach for fibre-reinforced composites design. International Journal for Simulation and Multidisciplinary Design Optimization. 2008;**2**(1):1-9

[2] Okafor CE, Okafor EJ, Obodoeze JJ, Ihueze CC. Characteristics and reliability of polyurethane wood ash composites for packaging and containerisation applications. Journal of Materials Science Research and Reviews. 2018;**1**(3):1-10

[3] Xie HB, Wang YF. Reliability analysis of CFRP-strengthened RC bridges considering size effect of CFRP. Materials. 2019;**12**(14):2247

[4] Beaumont PW, Soutis C, Hodzic A, editors. The Structural Integrity of Carbon Fiber Composites: Fifty Years of Progress and Achievement of the Science, Development, and Applications. Switzerland: Springer; 2016

[5] Pei X, Han W, Ding G, Wang M, Tang Y. Temperature effects on structural integrity of fiber-reinforced polymer matrix composites: A review. Journal of Applied Polymer Science. 2019;**136**(45):48206

[6] Bittrich L, Spickenheuer A, Almeida JHS, Müller S, Kroll L, Heinrich G. Optimizing variable-axial fiber-reinforced composite laminates: The direct fiber path optimization concept. Mathematical Problems in Engineering. 2019;**2019**:1-11

[7] Prasad SV, Kumar GA, Sai KP, Nagarjuna B. Design and optimization of natural fibre reinforced epoxy composites for automobile application. In: AIP Conference Proceedings. Vol. 2128(1). Melville, NY, USA: AIP Publishing; 2019. p. 020016

[8] Wang Y, Cui G, Shao Z, Bao Y, Gao H. Optimization of the hot pressing process for preparing flax fiber/PE thermoplastic composite. Mechanical Engineering Science. 2019;**1**(1):41-45

[9] Foulc MP, Bergeret A, Ferry L, Ienny P, Crespy A. Study of hygrothermal ageing of glass fibre reinforced PET composites. Polymer Degradation and Stability. 2005;**89**(3):461-470

[10] Shettar M, Chaudhary A, Hussain Z, Kini UA, Sharma S. Hygrothermal studies on GFRP composites: A review. In: MATEC Web of Conferences. Vol. 144. Karnataka, India: EDP Sciences; 2018. p. 02026

[11] Ngo TD. Natural fibers for sustainable bio-composites. In: Natural and Artificial Fiber-Reinforced Composites as Renewable Sources. Rijeka: IntechOpen; 2018. p. 107

[12] Rahmani H, Najaf SHM, Ashori A, Golriz M. Elastic properties of carbon fibre-reinforced epoxy composites. Polymers and Polymer Composites. 2015;**23**(7):475-482

[13] Schürmann H. Konstruieren mit Faser-Kunststoff-Verbunden. Berlin Heidelberg: Springer-Verlag; 2007

[14] Younes R, Hallal A, Fardoun F, Chehade FH. Comparative review study on elastic properties modeling for unidirectional composite materials. In: Hu N, editor. Composites and their Properties. London: IntechOpen; 2012

[15] Goncalves R, Trinca AJ, Pellis BP. Elastic constants of wood determined by ultrasound using three geometries of specimens. Wood Science and Technology. 2014;**48**:269-287

[16] Longo R, Delaunay T, Laux D, El Mouridi M, Arnould O, Le Clézio E. Wood elastic characterization from a

single sample by resonant ultrasound spectroscopy. Ultrasonics. 2012;**52**: 971-974

[17] Majano-Majano A, Fernandez-Cabo JL, Hoheisel S, Klein MA. Test method for characterizing clear wood using a single specimen. Experimental Mechanics. 2012;**52**:1079-1096

[18] Vazquez C, Gonçalves R, Bertoldo C, Bano V, Vega A, Crespo J, et al. Determination of the mechanical properties of *Castanea sativa* mill. using ultrasonic wave propagation and comparison with static compression and bending methods. Wood Science and Technology. 2015;**49**:607-622

[19] Adewole S. Plantain (*Musa acuminata*) value chain analysis in Ondo State, Nigeria. Scientific Papers: Management, Economic Engineering in Agriculture & Rural Development. 2017;**17**(3):25-36

[20] Widsten P, Kandelbauer A. Adhesion improvement of lignocellulosic products by enzymatic pre-treatment. Biotechnology Advances. 2008;**26**:379

[21] Ojediran EO, Ibrahim HK, Adebisi LO, Belewu KY, Owolawi S. Analysis of profitability and determinants of plantain production in IFE agricultural development project (ADP) zone of Osun state, Nigeria. Fuoye Journal of Agriculture and Human Ecology. 2017;**1**(1):77-86

[22] HTA. Constraints to Banana Production. Ibadan, Nigeria: International Institute of Tropical Agriculture; 1990. pp. 142-144

[23] Norgrove L, Hauser S. Improving plantain (Musa spp. AAB) yields on smallholder farms in West and Central Africa. Food Security. 2014;**6**(4):501-514

[24] Akinyemi SOS, Aiyelaagbe IOO, Akyeampong E. Plantain (Musa spp.)

cultivation in Nigeria: A review of its production, marketing and research in the last two decades. In: Dubois T, Hauser S, Staver C, Coyne D, editors. Proceedings of an International Conference on Banana & Plantain in Africa Harnessing International Partnerships to Increase Research Impact. Acta Horticulturae. Vol. 879. 2010. pp. 211-218

[25] Kaine AIN, Okoje LJD. Estimation of cost and return of plantain production in Orhionwon Local Government Area, Edo State, Nigeria. Asian Journal of Agriculture and Rural Development. 2014;**4**(2):162-168

[26] Kainga PE, Nnadi CD, Jimmy SP, Ugorji KS. Economics of plantain production in oil producing communities of Bayelsa State, Nigeria. Nigerian Journal of Agricultural Economics. 2015;**5**(1):54-60

[27] Ahmed S. The Survey of Nigeria Agriculture by Raw Materials Research and Development Council (RMRDC). 2004:123

[28] Olumba CC. Productivity of improved plantain technologies in Anambra State, Nigeria. African Journal of Agricultural Research. 2014;**9**(29): 2196-2204

[29] Samuel OD, Agbo S, Adekanye TA. Assessing mechanical properties of natural fiber reinforced composites for engineering applications. Journal of Minerals and Materials Characterization and Engineering. 2012;**11**(1):1-5

[30] Cadena Ch EM, Vélez R, M J, Santa JF, Otálvaro G. Natural fibers from plantain pseudostem (*Musa paradisiaca*) for use in fiber-reinforced composites. Journal of Natural Fibers. 2017;**14**(5):678-690

[31] Adeniyi AG, Ighalo JO, Onifade DV. Banana and plantain fiber-reinforced

polymer composites. Journal of Polymer Engineering. 2019;**39**(7):597-611

[32] Chimekwene CP, Fagbemi EA, Ayeke PO. Mechanical properties of plantain empty fruit bunch fiber reinforced epoxy composite. International Journal of Research in Engineering, IT and Social Sciences. 2012;**2**(6):86-94

[33] Okafor EC, Ihueze CC, Nwigbo SC. Optimization of hardness strengths response of plantain fibers reinforced polyester matrix composites (PFRP) applying Taguchi robust design. International Journal of Science & Emerging Technologies. 2013;**5**(1):1-11

[34] Alvarez-López C, Rojas OJ, Rojano B, Ganán P. Development of self-bonded fiberboards from fiber of leaf plantain: Effect of water and organic extractives removal. BioResources. 2014;**10**(1):672-683

[35] Obijiaku JC, Kamalu CIO, Osoka EC, Onyelucheya OE, Uzondu FN, Obibuenyi JI. Effects of extraction techniques on the yield and mechanical properties of empty plantain fruit bunch fibers. International Journal of Engineering and Management Research (IJEMR). 2015;**5**(6):494-500

[36] Ihueze CC, Okafor CE. Optimal design for flexural strength of plantain fibers reinforced polyester matrix. Journal of Innovative Research in Engineering and Sciences. 2016;**4**(4): 520-537

[37] Ihueze CC, Okafor EC. Response surface optimization of the impact strength of plantain fiber reinforced polyester for application in auto body works. Journal of Innovative Research in Engineering and Science. 2014;**4**:505-520

[38] Okafor CE, Godwin HC. Evaluation of compressive and energy adsorption characteristics of plantain fiber reinforced composites. World Journal of Engineering and Physical Sciences. 2014;**2**(3):036-048

[39] Oreko BU, Otanocha OB, Emagbere E, Ihueze CC. Analysis and application of natural fiber reinforced polyester composites to automobile fender. Covenant Journal of Engineering Technology (Special Edition). 2018;**1**(1): 1-12

[40] Imoisili PE, Tonye DI, Victor PA, Elvis OA. Effect of high-frequency microwave radiation on the mechanical properties of plantain (*Musa paradisiaca*) fibre/epoxy biocomposite. Journal of Physical Science. 2018;**29**(3):23-35

[41] Imoisili PE, Fadare OB, Popoola AV, Okoronkwo AE. Effect of chemical treatment on the morphology and mechanical properties of plantain (*Musa paradisiaca*) fibre. IOSR Journal of Applied Chemistry. 2017;**10**(5):70-73. DOI: 10.9790/5736-1005017073

[42] Sinebe JE, Chukwuneke JL, Omenyi SN. Implications of interfacial energetics on mechanical strength of fiber reinforced polymer matrix. International Journal of Materials Engineering. 2019;**9**(1):1-7. DOI: 10.5923/j.ijme.20190901.01

[43] Ihueze CC, Okafor CE, Okoye CI. Natural fiber composite design and characterization for limit stress prediction in multiaxial stress state. Journal of King Saud University-Engineering Sciences. 2015;**27**(2):193-206

[44] Kenedi PP, Vignoli LL, Duarte BT, Matos FCDA, Dias HOT. Orthotropic elastic properties assessment of sandwich laminates. Journal of Aerospace Technology and Management. 2017;**9**(3):389-396

[45] Hwang SF, Liu HT. Prediction of elastic constants of carbon fabric/polyurethane composites. In: Solid State Phenomena. Vol. 258. Baech,

Switzerland: Trans Tech Publications; 2017. pp. 233-236

[46] Ren B, Noda J, Goda K. Effects of fiber orientation angles and fluctuation on the stiffness and strength of sliver-based green composites. Journal of the Society of Materials Science, Japan. 2010;**59**(7):567-574

[47] Kumar KV, Reddy PR, Shankar DR. Influence of angle ply orientation of stacking on mechanical properties of glass-polyester composite laminate. International Journal of Engineering and Advanced Technology (IJEAT). 2013; **2249**:8958

[48] Cordin M, Bechtold T, Pham T. Effect of fibre orientation on the mechanical properties of polypropylene–lyocell composites. Cellulose. 2018;**25**(12):7197-7210

[49] Ihueze CC, Okafor EC, Ujam AJ. Optimization of tensile strengths response of plantain fibers reinforced polyester composites (PFRP) applying Taguchi robust design. Innovative Systems Design and Engineering. 2012; **3**(7):64-76

[50] Jules EJ, Tsujikami T, Lomov SV, Verpoest I. Effect of fibres length and fibres orientation on the predicted elastic properties of long fibre composites. Macromolecular Symposia. 2004;**17**:1-109

[51] Venetis J, Sideridis E. Elastic constants of fibrous polymer composite materials reinforced with transversely isotropic fibers. AIP Advances. 2015; **5**(3):037118

[52] Cuartas VM, Perrin M, Pastor ML, Welemane H, Cantarel A, Karama M. Determination of the elastic properties in CFRP composites: Comparison of different approaches based on tensile tests and ultrasonic characterization. Advances in Aircraft and Spacecraft Science. 2015;**2**(n° 3):249-260

[53] Clyne TW, Hull D. An Introduction to Composite Materials. Cambridge, United Kingdom: Cambridge University Press; 2019

[54] Datoo MH. Mechanics of Fibrous Composites. New York: Elsevier Science Publishing Co. Inc; 2012

[55] Maheshwari P, Misra A, Kumar A. Investigate the variation in elastic constants and failure strength of lamina with FVF and FOA for JFRP lamina. International Journal of Applied Engineering Research. 2018;**13**(9): 157-161

[56] Jones RM. Mechanics of Composite Materials. 2nd ed. Philadelphia, PA: Taylor and Francis, Inc.; 1999

[57] Gibson RF. Principles of Composite Material Mechanics. 4th ed. Boca Raton, FL: CRC Press; 2016

[58] Farooq U, Myler P. Efficient determination of mechanical properties of carbon fibre-reinforced laminated composite panels. ARPN Journal of Engineering and Applied Sciences. 2017; **12**(5):1375-1392

[59] Koussios S, Beukers A. Lekhnitskii's formalism for stress concentrations around irregularities in anisotropic plates: Solutions for arbitrary boundary conditions. In: Variational Analysis and Aerospace Engineering. New York, NY: Springer; 2009. pp. 243-265

[60] Lekhnitskii SG. Anisotropic Plates. 2nd ed. London, UK: Gordon and Breach; 1968